Electronic Supplementary Material (ESI) for ChemComm.

Electronic Supporting Information

Surface confined heteroleptic Copper(II)-polypyridyl complexes for photo-nuclease activity

Vikram Singh,[a] Prakash C. Mondal,[ab] Anup Kumar,[a] Yekkoni J. Lakshmanan,[c] Satish K. Awasthi,[a] Rinkoo D. Gupta,*[d] and Michael Zharnikov*[c]

[a] Department of Chemistry, University of Delhi, Delhi-110007, India

[b] Weizmann Institute of Science, Rehovot-76100, Israel

[c] Applied Physical Chemistry, University of Heidelberg, Im Neuenheimer Feld 253, D-69120 Heidelberg, Germany

[d] Faculty of Life Sciences and Biotechnology, South Asian University, Delhi-110021, India

Materials and methods:

4-pyridine carboxaldehyde, 1-10, phenanthroline monohydrate, 3-iodo-n-propyl-trimethoxysilane and sodium perchlorate were purchased from Sigma-Aldrich and were used as received. Glacial Acetic acid, copper acetate monohydrate were purchased from s. d. fine chemicals (India). Methanol was purchased from Merck and was distilled over activated magnesium turnings and iodine before use. 30% aq. Ammonia, H_2O_2, dry n-pentane, toluene, dichloromethane and acetonitrile (All AR grade) were purchased from s. d. fine chemicals (India). Glass slides having thickness ~1.0-1.2 mm were purchased from Pearl India and Single-crystal silicon [100] substrates were purchased from Georg Albert PVD- Beschichtungen (Silz, Germany). Hydrothermal bombs (25mL & 50mL) were purchased from Prakash Scientific Works (India). Water used for the experiment was double distilled.

Glass slides were cleaned by immersing them in *piranha* solution (7:3 (v/v)), Conc.H_2SO_4: 30% H_2O_2) for 1h and subsequent washing with ample amount of de-ionized (DI) water. (*Caution: Piranha is an extremely strong and dangerous oxidising agent and all protective measures must be adopted to prevent any harm.)* Then the slides were kept in RCA solution (1:5:1 (v/v), aq. NH_3:H_2O:H_2O_2) for 1h followed by rinsing with ample amount of de-ionized water, dried with N_2 stream and kept in oven for 2h at 110 ^{0}C. Silicon wafers were cleaned by sonication for 15 minutes each in n-hexane, acetone and isopropanol followed by drying under N_2 stream before placing in oven at 110 ^{O}C for 2h. The monolayer formation was carried out under an inert atmosphere using standard Schlenk/cannula techniques.

Physical measurements:

All ^{1}H NMR spectra were recorded on Jeol JNMECX 400P spectrometer. Infrared spectra were recorded on Perkin-Elmer FT-IR spectrometer. Elemental analyses were performed on a GMbH VarioEL elemental analyzer. All the above data collection was performed at

Central Instrumentation Facility (CIF), University of Delhi. Electronic absorption spectra were recorded using JASCO UV-Vis-NIR spectrophotometer (Model 660D). Mass spectra were recorded on THERMO Finnigan LCQ Advantage max ion trap mass spectrometer (MSAIF, CDRI, Lucknow, India).

Synthesis of ligands:

Ligand 1: 2-(anthracen-9-yl)-1H-imidazo[4,5-f][1,10]phenanthroline[S1]

Ligand 2: 2-(pyren-1-yl)-1H-imidazo[4,5-f][1,10]phenanthroline[S1]

Ligand 3: 2-(4-pyridyl)-1H-imidazo[4,5-f][1,10]phenanthroline[S2]

1,10-phenanthroline-5,6-dione (PD) was synthesized from reported procedures. 0.15 g (0.714 mmol) of PD and 1.75 g (22 mmol) of NH_4OAc were taken and to this was added 10 mL of glacial acetic acid. The solution was refluxed at 80 ^oC until the mixture dissolves. Then, 0.714 mmol of respective aldehyde in 7 mL of glacial acetic acid was added to the hot solution. The color changed to deep red while addition and refluxed for further 3 hours. The solution was cool down to room temperature, neutralized by 30 % aq. NH_3 solution during which a yellowish orange precipitate was observed. The precipitate was filtered, washed with cold H_2O and dried *in vacuo*.

Ligand 1: ^1H NMR (400 MHz, DMSO-d_6): δ 14.30 (s, 1H (N-H)); δ 9.12 (dd, *J* = 6.45 Hz, *J* = 2.97 Hz, 2H); 9.04 (d, *J* = 10 Hz, 2H); δ 8.92 (s, 1H); δ 8.28 (d, *J* = 8.6 Hz, 2H); δ 7.82 (m, 4H); δ 7.58 (m, 4H). Yield: 28%. ESI-MS (+ve mode): *m/z* 397 $(M + H)^+$; 419 $(M + Na)^+$.

Ligand 2: ^1H NMR (400 MHz, DMSO-d_6): δ 14.10 (s, 1H (N-H)); δ 9.51 (d, J = 9.3 Hz, 1H); δ 9.08 (dd, 2H); δ 8.66 (d, J = 8.1 Hz, 1H); δ 8.52 (d, J = 8.48 Hz, 1H); δ 8.30 (m, 8H); δ 7.88 (dd, J = 8.0 Hz, J = 3.89 Hz, 2H). ESI-MS (+ve mode): *m/z* 421$(M + H)^+$; 443 $(M + Na)^+$.

Ligand 3: ^1H NMR (400 MHz, DMSO-d_6): δ 9.17 (m, 2H); δ 8.90 (m, 4H); δ 8.23 (m, 2H); δ 7.95 (m, 2H). ESI-MS (+ve mode): m/z 298 $(M + H)^+$.

Synthesis of Complexes 1 and 2:

74 mg (0.02 mmol) of $Cu(ClO_4)_2.6H_2O$ is dissolved in 10 mL of MeOH at room temperature. To the stirred solution, added drop-wise a 0.02 mmol of ligand (1 or 2) in 10 mL of MeOH. The solution was stirred for 2 h and then 59.4 mg (0.02 mmol) of ligand 3 in 10 mL of MeOH was added drop-wise to the stirred solution. Further stirring for 1 h afforded a light to dark green colored precipitate. The precipitate was washed with ether and dried over anhydrous calcium chloride and kept in glovebox. Yield: ~ 50-60%.

Complex 1: Solubility: Soluble in DMF, DMSO, soluble in DMF/water mixture (10% DMF), less soluble in CH_3CN, very less soluble in Ethanol. ATR-IR (ν_{max}, cm^{-1}): 3224 (w) (2^o N-H), 3083 (aromatic C-H), 1616, 1566 (m) (C=C), 1411 (m) (C=N), 1091 (vs) (Cl-O), 839 (m), 726 (m). UV-Vis (10^{-5} M in 10% DMF) (λ_{max}, logε): 296 nm, 4.53; 363 nm, 4.28; 383 nm, 4.26; 600 nm, 2.10. $\lambda_{excitation}$ = 283 nm, $\lambda_{emission}$ = 350 nm: Quantum yield, Φ = 0.022 $(Ru(bpy)_3^{2+}$ as standard reference at 25 $^oC)$[S3]. (ESI-MS (+ve mode): *m/z* 378 (M^+) [$M^+ = (M^{2+} - 2ClO_4) / 2$]. Anal. Calcd. for $C_{45}H_{27}N_8O_8Cl_2Cu.H_2O$: C, 55.48; H, 3.00; N, 12.94. Found C, 55.26; H, 2.81; N, 12.71 (%).

Complex 2: Solubility: Soluble in DMF, DMSO, soluble in DMF/water mixture (10% DMF), less solubility in CH_3CN, very little solubility in Ethanol. ATR-IR (ν_{max}, cm^{-1}: 3224 (w) (2^o N-H), 3098 (w) (aromatic C-H), 1613 (C=C), 1091 and 1061 (vs) (Cl-O) , 839 (m), 697(w). UV-Vis (10^{-5} M in 10% DMF) (λ_{max}, logε): 294 nm, 4.09; 316 (sh), 3.87; 364 (sh), 3.87; 646 nm, 1.04. $\lambda_{excitation}$ = 290 nm, $\lambda_{emission}$ = 365 nm: Quantum yield, Φ = 0.029 $(Ru(bpy)_3^{2+}$ as standard reference at 25 $^oC)$[S3]. ESI-MS (+ve mode): m/z 390 (M^+)[$M^+ = M^{2+} - (ClO_4)_2$]. Anal. Calcd. for $C_{47}H_{27}N_8O_8Cl_2Cu.H_2O$: C, 56.55; H, 2.93; N, 12.63. Found C, 56.32; H, 2.70; N, 12.42 (%).

Fabrication of monolayers of 1 and 2 (M1 and M2 respectively):

The freshly cleaned glass slides (2.5 × 0.9 × 0.1 cm^3) and silicon wafers (1.0 × 1.2 cm^2) were immersed in the solution of complex **1** and **2** (0.5 mM, acetonitrile/toluene

(v/v), 3:7) in a Teflon pressure vessel under N_2 atmosphere using Schlenk/cannula techniques. The vessel was kept in a programmed oven for 52h at 85 ^oC. The reaction vessels were then cooled to room temperature and the functionalised substrates were rinsed with acetonitrile and dichloromethane. Further, these substrates were sonicated for 3 minutes each in acetonitrile and isopropanol. The substrates were then dried and stored in desiccator with exclusion of light and under inert atmosphere. Increasing the reaction time from 52 to 64h does not affect the intensity and peak position of the MLCT bands at λ_{max} = 372 nm and 379 nm for **M1** and **M2** monolayer respectively, indicating the formation of a fully formed monolayer. Shortening the monolayer deposition time to 20 h decreases the intensity (~20-25%) of the absorption band in both cases.

Absorption spectral titrations (1 *vs* ct-DNA and 2 *vs* ct-DNA):

In absorption spectral titrations (AST), fixed aliquots of ct-DNA in 50 mM tris HCl/NaCl buffer (pH = 7.2) were added to 10 μM (DMF:H_2O :: 1:9 (v/v)) solutions of 1 and 2 and optical absorption was recorded after 5 minute equilibration time and 200 nm min^{-1} scan speed, until there were no further alterations in the optical absorption. Equal quantity of ct-DNA was added to the reference side as well so as to nullify the effect of DNA absorption. Interpretation and subsequent calculation of binding parameters from UV/Vis data was followed after due volume corrections. Intrinsic binding constant, K_b was calculated using McGhee von Hippel equation[S4] (1),

$$[DNA]/(\varepsilon_a - \varepsilon_f) = [DNA]/(\varepsilon_b - \varepsilon_f) + 1/K_b(\varepsilon_b - \varepsilon_f) \ldots\ldots\ldots (\mathbf{1})$$

where, ε_f, ε_b, ε_a are the molar extinction coefficients of the free complex, of fully bound complex, and at addition of each aliquot of DNA (apparent), respectively. [DNA] is the concentration of ct-DNA in base pairs. $\boldsymbol{\varepsilon_a}$ can be calculated using A_{obs}/[Complex],[S5] where A_{obs} is absorbance of the complex and [Complex] is the dilution corrected concentration of the complex after each addition of aliquot of DNA. Expression of Bard and coworkers[S6] (modified MvH equation) (**2**) and **(3)** was used for calculating binding site size, '*s*' in base pairs.

$$\Delta\varepsilon_{af} / \Delta\varepsilon_{bf} = (b - (b^2 - 2K_b^2C_t[DNA]/s)^{1/2})/2K_bC_t \text{.....(2)}$$

$$\text{where } b = 1 + K_bC_t + K_b[DNA]/2s \text{.....(3)}$$

Number of binding sites per molecule, Γ_{max} ccould be calculated using equation (**4**),[S7]

$$\Gamma_{max} = 1/2s \text{.....(4)}$$

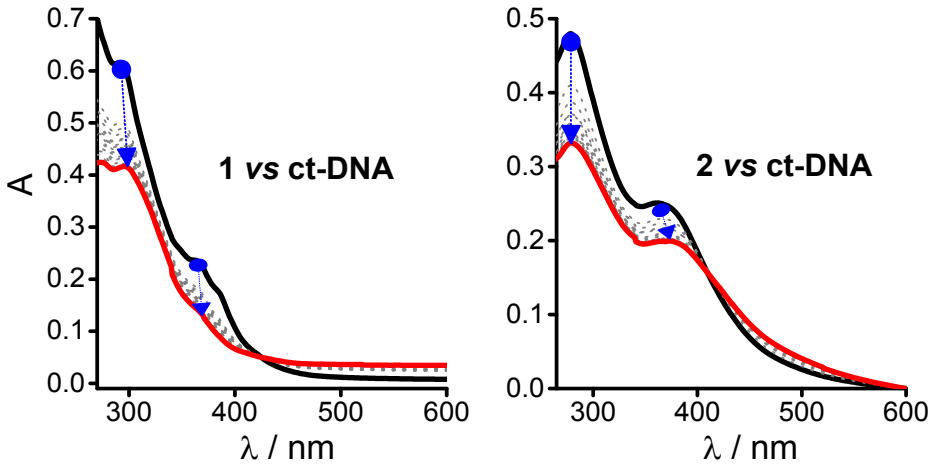

Figure S1. Absorption spectral traces of 10^{-5} M of **1** (left) and **2** (right) in 10% DMF, upon gradual addition of ct-DNA (300 µM) in 50 mM tris-HCl buffer. Black curve indicate UV/Vis spectrum of free complex; dotted lines indicate gradual addition of DNA to respective complex and red line indicate saturation point. Blue arrows indicate extent of hypochromic (30 and 31% for complex **1** (w.r.t λ_{max} = 294 nm) and **2** (w.r.t λ_{max} = 280 nm) respectively) and bathochromic shifts (5 and 12 nm for complex 1 (w.r.t λ_{max} = 367 nm) and 2 (λ_{max} = 365 nm) respectively).

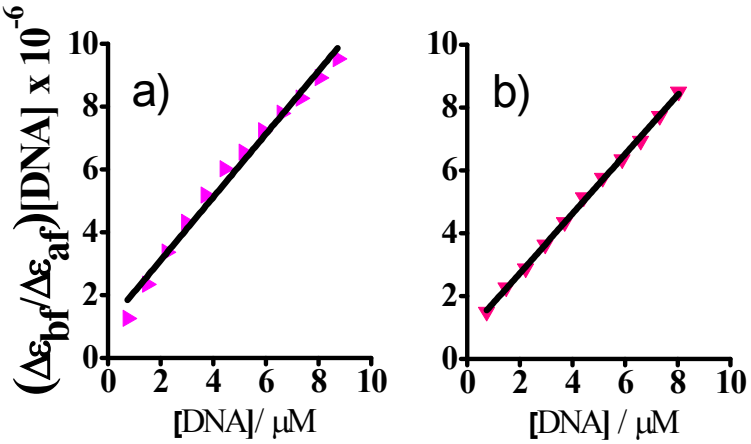

Figure S2. Linear least square fits of ($\Delta\varepsilon_{bf}$ / $\Delta\varepsilon_{af}$) x [DNA] vs. [DNA] using the MvH equation. a) **1** (R^2 = ~0.983) and b) **2** (R^2 = ~0.998).

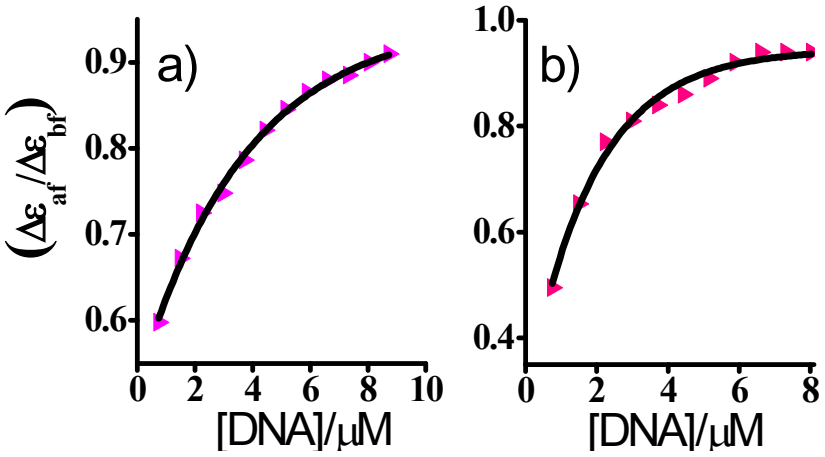

Figure S3. Non- linear least square fitted graphs from modified MvH equation for complexes **1** and **2**. a) **1** (R^2 = ~0.996) and b) **2** (R^2 = ~0.987).

Table S1. Absorption spectral titration characteristics.

Complex	K_b / M^{-1}	*s* / bp	Binding sites per molecule / Γ_{max}
1	**9.09×10^5**	**0.071**	**7.04**
2	**1.19×10^6**	**0.087**	**5.74**

Fluorescence Studies:

A solution of 2 mL of 1.3 μM of EB prepared in 50 mM tris HCl/NaCl buffer was excited at 501 nm and emission was recorded at 601 nm. 10 μL aliquots of 300 μM ct-DNA were subsequently added to EB solution resulting in enhancement of fluorescence intensity (measured at same excitation and emission wavelengths), until there were no further changes (Fig. 1). The experiment was performed three times under identical conditions and after subtracting the value of the baseline (Tris HCl buffer), the fluorescence value '*F*', at λ_{max} = 601 nm was corrected for dilutions using equation **5**.

$$F_{corr} = F \times (2000 + X) / 2000 \ldots\ldots\ldots\ldots (\mathbf{5})$$

where 'F_{corr}' is the corrected fluorescence value, 2000 is mixture volume in microlitres before DNA addition and X is the volume of DNA solution added. A quantity '*f*' (equation **6**) was used to represent fraction of EB bound to DNA. Scatchard method[S8-S10] as

described by Healy[S11] was employed for fitting the collected data for three sets within experimental error limits (Fig. 1) (equation **7**).

$$f = (F_{corr} - F_o / F_{max(corr)} - F_o) \text{.....} (\mathbf{6})$$

$$[DNA]/f = (N / K_{EB}) \times (1 - f)^{-1} + N \times [EB] \text{.....} (\mathbf{7})$$

where 'N' is the number of base pairs per molecule of EB and K_{EB} is EB-DNA binding constant. K_{EB} and 'N' were calculated to be 1.05 x 10^7 M^{-1} and ~ 2.5 base pairs which is well within the error limits of the reported value.

To this EB-Bound DNA solution, increasing aliquots of 1 mM stock solutions of various copper complexes were added in separate experiments, and at similar excitation and emission wavelengths, continuous fluorescence quenching was observed for each complex. Apparent binding constant, K_{app} for complexes were calculated using equation **8**.[S12]

$$K_{EB} \times [EB] = K_{app} \times DC_{50} \text{.....} \mathbf{(8)}$$

where, [EB] = 1.3 μM and DC_{50} is the concentration of complex at 50 % EB displacement.

To quantitatively correlate fluorescence quenching to the concentration of the quencher, that is, copper complexes, fluorescence data were transformed into Stern–Volmer plots according to Stern–Volmer equation **9** for collisional/dynamic quenching.[S13]

$$F_0/F = 1 + K_{sv} \times [Q] \text{.....} (\mathbf{9})$$

where F_0 and F are the fluorescence area in the absence and presence of the quencher, [Q] is the ratio of the concentration of the copper complexes to DNA and K_{sv} is the Stern-Volmer quenching constant and is the measure of accessibility of the copper complexes to the EB-DNA intercalating sites.[S14]

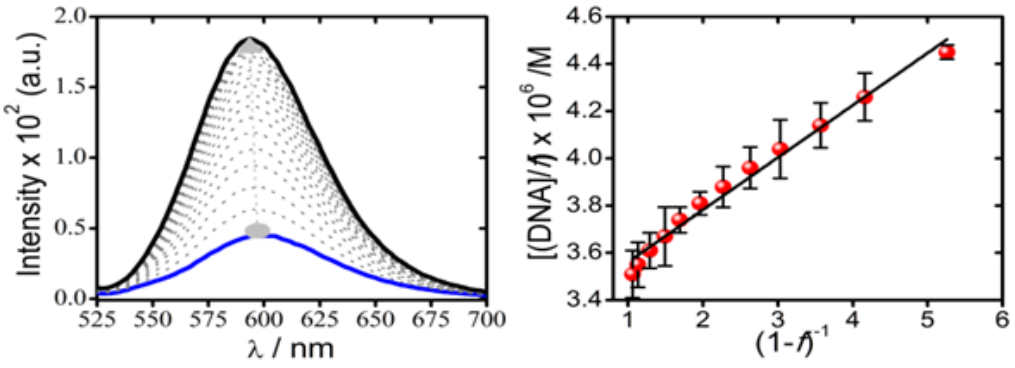

Figure S4. (Left) Blue line: fluorescence of EB in tris HCl buffer solution; To this EB solution, aliquots of DNA were added resulting in gradual increase in fluorescence with saturation shown by black line. (Right) Scatchard plot for calculating K_{EB} (linear least square fitting; R^2 = ~0.99).

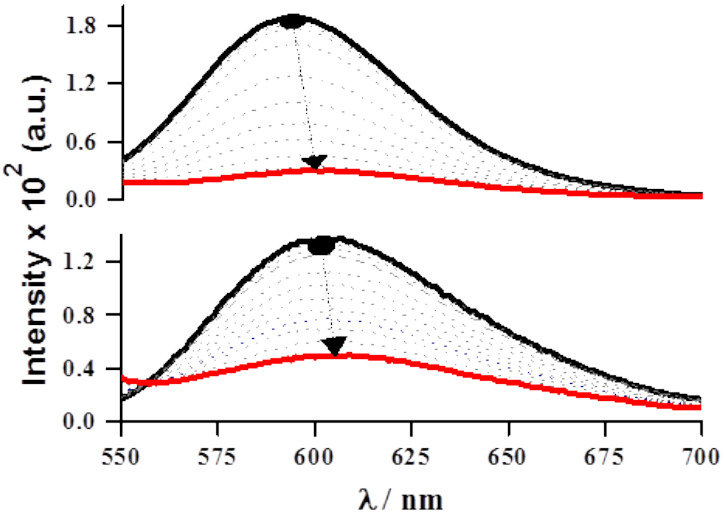

Figure S5. Gradual addition of complex **1** (top) and complex **2** (bottom) to EB bound DNA leading to quenching of fluorescence as shown through black arrow.

Photonuclease activity:

At first a control study was performed where samples were not irradiated with UV-A light (365 nm, 12 W). Samples were prepared using 10 μM of each of the complex in glass vials. To this was added to 0.5 μL of pUC19 DNA (from 250μg/mL solution). After mixing them using a spinner, the samples were incubated for 1.5 h at 37.5 ^{o}C under dark conditions. After incubation, 2 μL of loading buffer, containing 25% bromophenol blue, 0.25% xylene cyanol, and 30% glycerol, was added to each sample and spinned to mix. Gel electrophoresis was

performed using BioRAD PowerPac Basic and BioRAD mini sub-cell GT with 10 µL of incubated sample under optimized conditions of 0.8 % agarose gel, potential was maintained at 40V, 2h running time and dark conditions in 1X tris acetate-EDTA (TAE) buffer. The bands were photographed using BioRAD molecular imaging ChemiDoc XRS+. In the main experiment, samples were irradiated with UV-A light (365 nm, 12 W) for 0.5 h and 1h and were incubated at 37.5 ^{o}C for 1 h under dark conditions. Gel-electrophoresis and documentation was performed under similar conditions as mentioned above.

Mechanistic experiments:

Number of control experiments were performed by using 5 µL of 5 mM each of NaN_3 ($^1O_2$ quencher), D_2O ($^1O_2$ lifetime enhacer), DMSO (OH· Scavenger), KI (O_2^{2-} and OH· Scavenger). These were added prior to the addition of the respective complex. Gel-electrophoresis was performed under similar conditions as mentioned above.

Following the above procedure, photo nuclease activity of the complex **1** and **2** was ascertained and percent of DNA cleavage (C) was calculated using equation 10.[S1]

$$C = ([\text{Form II}] + 2[\text{Form III}]) / ([\text{Form I}] + [\text{Form II}] + 2[\text{Form III}]) \quad (\mathbf{10})$$

where Form I represents supercoiled DNA (SC DNA), Form II represents nicked circular DNA (NC DNA) and Form III represents Linear DNA. Corrections were made to 'C' for presence of low level of nicked DNA in uncut plasmid and also low level of affinity of EB binding to supercoiled compared to nicked circular and linear forms of DNA. % DNA cleavage given in this study for each set of experiment is the mean of three separate experiments performed under similar conditions.

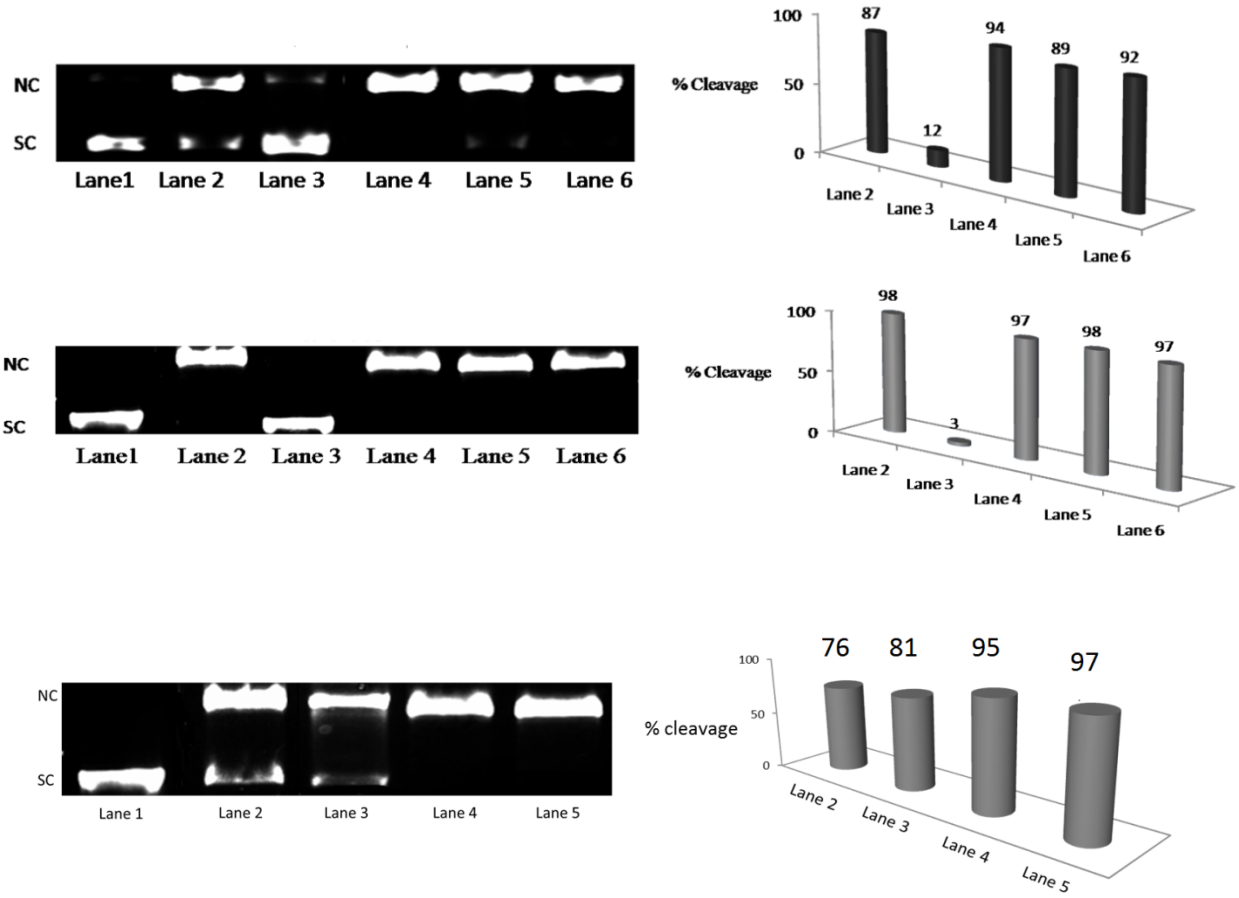

Figure S6. (Left) Photonuclease activity of10μM of complex **1** (Top) and complex **2** (middle) from lane 1 to lane 6. Lane 1: DNA control, Lane 2: DNA + **1**/**2**+ UV light, Lane 3: DNA + **1**/**2**+ NaN_3 + UV light, Lane 4: DNA + **1**/**2** + D_2O + UV light, Lane 5: DNA + **1**/**2** + DMSO + UV light, Lane 6: DNA + **1**/**2** + KI + UV light. (Right) % cleavage observed under various controls. (Bottom) Effect of addition of D_2O to 7 μM of complex **1**/**2**. Lane 1: DNA control, Lane 2: DNA + **1** + UV light, Lane 3: DNA + **2** + UV light, Lane 4: DNA + **1** + D_2O + UV light, Lane 5 DNA + **2** + D_2O + UV light.

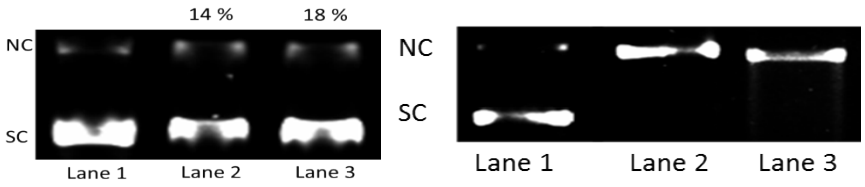

Figure S7. (Left) Photonuclease activity of ligand **1** and ligand **2** under similar conditions as for complexes **1** and **2** (% DNA cleavage is marked above). (Right) Photonuclease activity of complex **1** and **2** under N_2 atmosphere. Lane 1: DNA control, Lane 2: DNA + **1** + UV light + N_2 (~8% cleavage), Lane 3: DNA + **2** + UV light + N_2 (~11% cleavage).

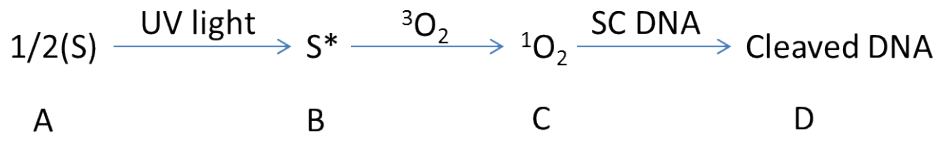

Figure S8. Mechanism for the generation of singlet oxygen and subsequent DNA cleavage. A) Complex 1/2 are irradiated with UV light at 365 nm leading to B) photosensitized state (S*), which transfer energy to non-toxic triplet oxygen to form C) highly toxic singlet oxygen, which cleave SC DNA to D) DNA fragments

XPS and NEXAFS measurements on M1 and M2:

The X-ray spectroscopy (XPS) and near-edge X-ray absorption fine structure (NEXAFS) spectroscopy measurements were performed at the HE-SGM beamline (bending magnet) of the synchrotron storage ring BESSY II in Berlin, Germany. XP spectra were acquired using a Scienta R3000 spectrometer. The synchrotron light served as the X-ray primary source. The spectra acquisition was carried out in normal emission geometry with an energy resolution of ~0.3-0.5 eV, depending on the photon energy. The energy scale of the XP spectra was referenced to the Au $4f_{3/2}$ peak at a binding energy (BE) 84.0 eV.[S15]

The acquisition of the NEXAFS spectra was carried out at the carbon and nitrogen K-edges in the partial electron yield mode with retarding voltages of -150 and -300 V, respectively. Linear polarized synchrotron light with a polarization factor of ~91% was used. The energy resolution was ~0.3 eV at the C K-edge and ~0.5 eV at the N K-edge. The incidence angle of the light was kept at 55° to avoid orientational effects[S16] which, however, were not expected in the studied films, based on our experience with similar systems. The raw C K-edge spectra were normalized to the incident photon flux by division by a spectrum of a clean, freshly sputtered gold sample. The photon energy scale was referenced to the most intense π^* resonance of highly oriented pyrolytic graphite at 285.38 eV.[S17]

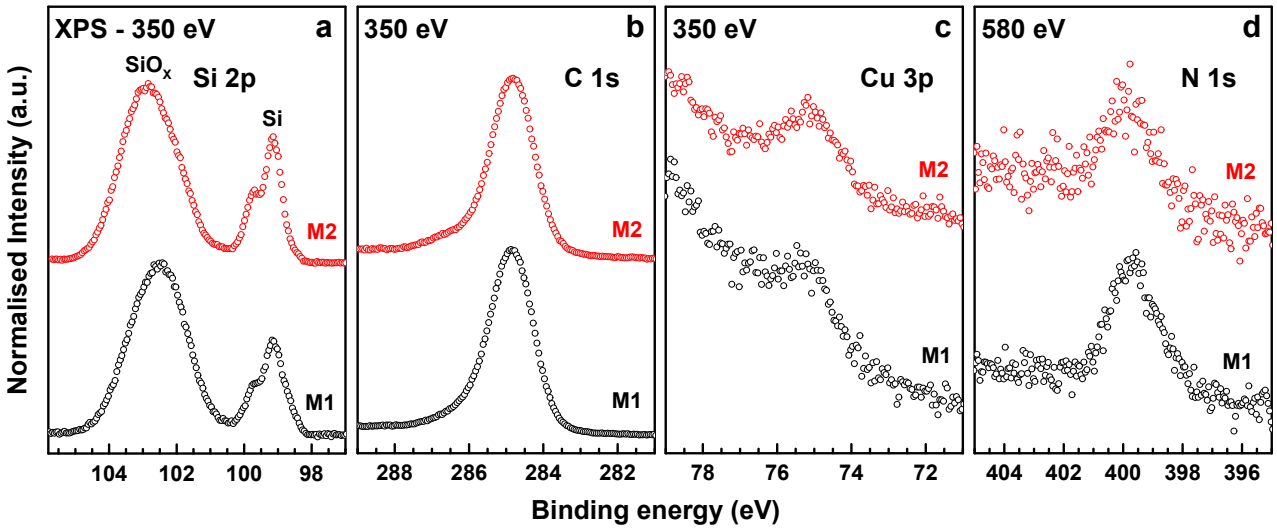

Figure S9. Si 2p (a), C 1s (b), Cu 3p (c), and N 1s (d) XP spectra of M1 (black) and M2 (red) on Si(100) acquired at photon energies of 350 and 580 eV, as marked in the panels. The spectra exhibit characteristic emissions associated with individual building blocks of **1** and **2**.

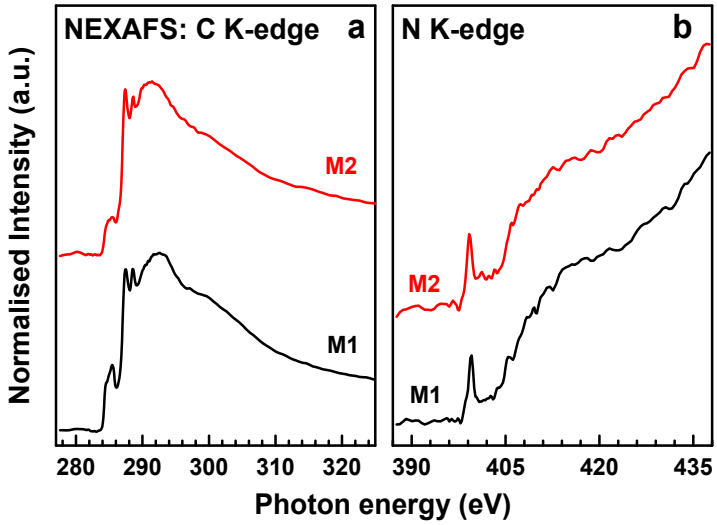

Figure S10. C (a) and N (b) K-edge NEXAFS spectra of of M1 (black) and M2 (red) on Si(100) acquired at an X-ray incidence angle of 55°. The spectra exhibit characteristic resonances associated with individual building blocks of **1** and **2**.

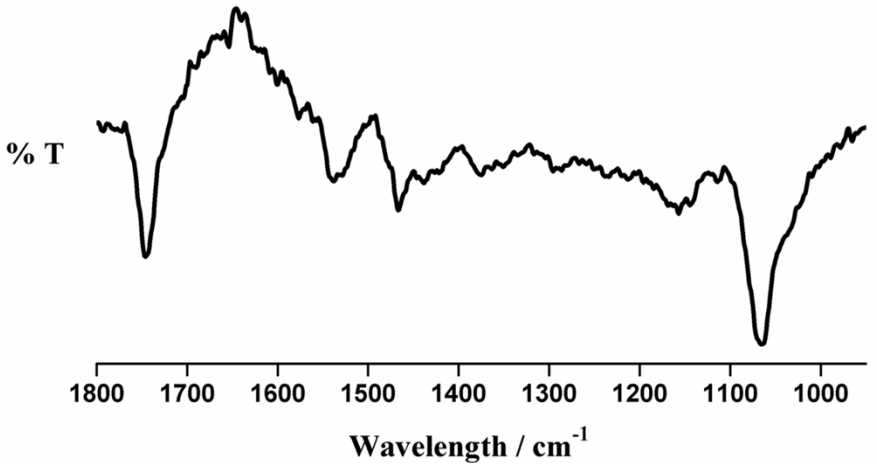

Figure S11: FT-IR spectra of ct-DNA in tris HCl/NaCl buffer. Baseline was recorded with tris HCl/NaCl buffer for preliminary adjustments. Relevant IR stretches are explained in the text.

References:

S1: M. Mariappan and B. G. Maiya, *Eur. J. Inorg. Chem.*, 2005, 2164.

S2: N. N. Sergeeva, M. D-. Marechal, G. Vaz, A. M. Davies, M. O. Senge, *J. Inorg. Biochem.*, 2011, **105**, 1589.

S3: J. F. Michalec, S. A. Bejune, D. G. Cuttell, G. C. Summerton, J. A. Gertenbach, J. S. Field, R. J. Haines and D. R. McMillin, Inorg. Chem., 2001, **40**, 2193.

S4: J. D. McGhee and P. H. V. Hippel, *J. Mol. Biol.*, 1974, **86**, 469.

S5: E. Sundaravadivel, M. Kandaswamy and B. Varghese, *Polyhedron*, 2013, **61**, 33.

S6: M. T. Carter, M. Rodriguez and A. J. Bard, *J. Am. Chem. Soc.*, 1989, **111**, 8901.

S7: W. Chen, N. J. Turro and D. A. Tomalia, *Langmuir*, 2000, **16**, 15.

S8: H. G. Weder, J. Schildknecht, R. A. Lutz and P. Kesselring, *Eur. J. Biochem.*, 1974, **42**, 475.

S9: J. G. Norby, P. Ottolenghl and J. Jensen, *Anal. Biochem.*, 1980, **102**, 318.

S10: K. Zierler, *Trends Biochem. Sci.*, 1989, **14**, 314.

S11: E. F. Healy, *J. Chem. Edu.*, 2007, **84**, 1304.

S12: M. Lee, A. L. Rhodes, M. D. Wyatt, S. Forrow and J. A. Hartley, *Biochemistry*, 1993, **32**, 4237.

S13: J. R. Lakowicz, Principles of Fluorescence Spectroscopy, 2nd edn., Kluwer Academic/Plenum Publishers, 1999.

S14: D. Sarkar, P. Das, S. Basak, N. Chattopadhyay, *J. Phys. Chem.*, 2008, **112**, 9243.

S15: J. F. Moulder, W. E. Stickle, P. E. Sobol, K. D. Bomben, Handbook of X-ray Photoelectron Spectroscopy, J. Chastian, Ed., Perkin-Elmer Corp.: Eden Prairie, MN, 1992.

S16: J. Stöhr, NEXAFS Spectroscopy; Springer Series in Surface Science 25; Springer-Verlag: Berlin, 1992.

S17: P. E. Batson, *Phys. Rev. B* 1993, **48**, 2608.